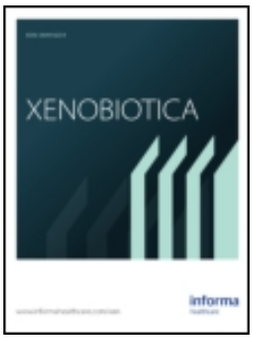

Xenobiotica
the fate of foreign compounds in biological systems

ISSN: 0049-8254 (Print) 1366-5928 (Online) Journal homepage: https://www.tandfonline.com/loi/ixen20

Morphological behaviour and metabolic capacity of cryopreserved human primary hepatocytes cultivated in a perfused multiwell device

Aurelie Vivares, Sandrine Salle-Lefort, Catherine Arabeyre-Fabre, Robert Ngo, Geraldine Penarier, Michele Bremond, Patricia Moliner, Jean-François Gallas, Gerard Fabre & Sylvie Klieber

To cite this article: Aurelie Vivares, Sandrine Salle-Lefort, Catherine Arabeyre-Fabre, Robert Ngo, Geraldine Penarier, Michele Bremond, Patricia Moliner, Jean-François Gallas, Gerard Fabre & Sylvie Klieber (2015) Morphological behaviour and metabolic capacity of cryopreserved human primary hepatocytes cultivated in a perfused multiwell device, Xenobiotica, 45:1, 29-44, DOI: 10.3109/00498254.2014.944612

To link to this article: https://doi.org/10.3109/00498254.2014.944612

Published online: 28 Jul 2014.

http://informahealthcare.com/xen
ISSN: 0049-8254 (print), 1366-5928 (electronic)

Xenobiotica

Xenobiotica, 2015; 45(1): 29–44
© 2015 Informa UK Ltd. DOI: 10.3109/00498254.2014.944612

informa
healthcare

RESEARCH ARTICLE

Morphological behaviour and metabolic capacity of cryopreserved human primary hepatocytes cultivated in a perfused multiwell device

Aurelie Vivares[1]*, Sandrine Salle-Lefort[1]*, Catherine Arabeyre-Fabre[1], Robert Ngo[1], Geraldine Penarier[2], Michele Bremond[3], Patricia Moliner[1], Jean-François Gallas[2], Gerard Fabre[1], and Sylvie Klieber[1]

[1]*Drug Disposition Domain, Disposition, Safety and Animal Research Scientific Core Plateform, SANOFI R&D, Montpellier, France,* [2]*Exploratory Unit, SANOFI R&D, Montpellier, France, and* [3]*Preclinical Safety Domain, Disposition, Safety and Animal Research Scientific Core Plateform, SANOFI R&D, Montpellier, France*

Abstract

1. The quantitative prediction of the pharmacokinetic parameters of a drug from data obtained using human *in vitro* systems remains a significant challenge i.e. prediction of metabolic clearance in humans and estimation of the relative contribution of enzymes involved in the clearance. This has become particularly problematic for low turnover compounds.
2. Having human hepatocytes with stable cellular function over several days that adequately mimic the complexity of the physiological environment would be a major advance. Thus, we evaluated human hepatocytes, maintained in culture during 7 days in the microfluidic LiverChip™ system, in terms of morphological appearance, relative mRNA expression of phase I and II enzymes and transporters as a function of time, and metabolic capacity using probe substrates.
3. The results showed that mRNA levels of the major genes for enzymes involved in drug metabolism were well-maintained over a 7-day period of culture. Furthermore, after 4 days of culture, in the Liverchip™ device, human hepatocytes exhibited higher or similar CYPs activities compared to 1 day of culture in 2D-static conditions.
4. The functional data were supported by light/electron microscopies and immunohistochemistry showing viable tissue structure and well-differentiated human hepatocytes: presence of cell junctions, glycogen storage, and bile canaliculi.

Keywords

Dynamic culture, drug metabolism, LiverChip™ device

History

Received 30 April 2014
Revised 7 July 2014
Accepted 10 July 2014
Published online 28 July 2014

Introduction

Human hepatocyte cultures, from either fresh or cryopreserved cells, are a widely accepted *in vitro* tool for studying drug metabolism, gene expression regulation and hepatotoxicity. Nevertheless, the current *in vitro* models used in pharmaceutical drug discovery and development laboratories are still limited in their predictive capability. Though the activity of Phase I and Phase II enzymes in these cellular systems are generally relatively well maintained over time scales required to obtain both quantitative and qualitative information on metabolic conversion, the analysis of slowly metabolically-cleared compounds and hepatotoxicity, which require longer culture times, can be extremely difficult. In fact, it is well established that primary hepatocytes rapidly de-differentiate in static monolayer culture, preventing accurate studies of drug metabolism and toxicity beyond a few hours or days (Meng, 2010). In particular, CYP-dependent activities significantly decrease during the first 24–48 h in monolayer culture. Moreover, static *in vitro* cell-based assays do not adequately mimic the complexity of the physiological environment and thus may not accurately reflect relevant human parameters. In this respect, much effort has been focused on developing more physiologically-relevant, long-term culture model systems for assessing hepatotoxicity, for *in vitro-in vivo* extrapolation (IVIVE) and for supporting development of physiologically-based pharmacokinetic models of drug disposition and toxicity with a paradigm shift to three-dimensional (3D) and/or perfused hepatocyte cultures (Dash et al., 2009; Godoy et al., 2013; Lecluyse et al., 2012). These approaches include the development of models based on co-culture of hepatocytes and non-parenchymental cells (Kaihara et al., 2000), sandwich hepatocyte cultures (Wang, 2008), 3D-liver tissue culture scaffolds (Bokhari et al., 2007), microfluidic systems (Baudoin et al., 2013; Fiegel et al., 2004; Novik et al., 2010) and self-assembling cellular spheroids (Messner et al., 2013).

*These authors contributed equally to the work.

Address for correspondence: Sylvie Klieber, Drug Disposition Domain, Disposition, Safety and Animal Research Scientific Core Plateform, SANOFI R&D, 371 Rue du Professeur Joseph Blayac, 34184 Montpellier, Cedex 4, France. Tel: 33 (0)4 99 77 54 95. Fax: 33 (0)4 99 77 54 91. E-mail: sylvie.klieber@sanofi.com

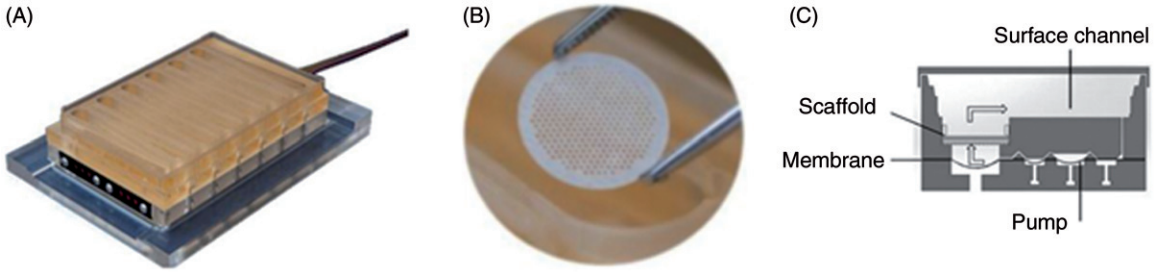

Figure 1. CN Bio Innovations LiverChip™ device. (A) The LiverChip™ system is an array of open-well bioreactors, each consisting of a reactor well, a reservoir well and an integrated pump. The reactor well contains a scaffold coated with collagen where cells self-assemble into an array of 3D microtissue unit; (B) 3D-scaffold; (C) schematic representation of the cross section of a bioreactor, the flow circulating through the scaffold and the bioreactor by the micropump (prints are a gift from CNBio innovations).

LiverChip™ device from CN Bio Innovations consists of a liver tissue-engineered perfused bioreactor and appear promising for studying drug toxicity and metabolism (Domansky et al., 2005). The core of the LiverChip™ device is composed of a scaffold (Figure 1A) containing a matrix of 3D-liver tissue that mimics the liver capillary bed. Culture medium continually circulates through the scaffold and bioreactor (Figure 1B). To enhance throughput as well as integration into existing automated cell culture paradigms, the device is designed to mimic the format of a multi-well plate, and houses twelve isolated bioreactors, each of them with an integrated micro pump for controlling flow (Figure 1C). The capillary bed is formed after seeding a suspension of liver cells into a reactor well; the cells adhere to the scaffold contained in the well and form tissue-like structures under continuous perfusion. As culture medium flows through the tissue bed, oxygen is consumed, resulting in a gradient across the tissue that is similar to the oxygen gradient in the *in vivo* liver sinusoid (Domansky et al., 2010). Rat hepatocytes cultured in these micro-reactors, maintain mRNA levels of the main cytochrome P450's and phase II enzymes over a seven day period of culture (Sivaraman et al., 2005). Finally, preliminary data obtained from human hepatocytes under the flow conditions of the LiverChip™ device seemed to provide a good extrapolated prediction of *in vivo* clearance (Dash et al., 2009; Maguire et al., 2009).

In this paper, we demonstrate the maintenance of the human hepatocyte phenotype in the LiverChip™ device by both, the characterization of the morphological behaviour of the cells and the analysis of mRNA basal expression of 22 genes involved in drug metabolism and transport over a seven day culture period. The results show that human hepatocytes, maintained for seven days in culture in the LiverChip™ device, exhibit a well-differentiated phenotype and in addition show a global preservation of mRNA expression levels of both metabolic and transporter genes. Moreover, preservation of metabolic capacity was evaluated over time, demonstrating that the clearance of five reference probe substrates, midazolam, dextromethorphan, phenacetin, bupropion and tolbutamide, was at least identical or higher after 7 days of culture in the dynamic LiverChip™ system than that after one day under 2D-static culture conditions. In addition to metabolic clearance, metabolite identification studies also demonstrated that the overall non CYP-dependent biotransformation processes implicated in the metabolism of the probes were present.

Materials and methods

Chemicals and reagents

The following drug substrates, metabolites and cell culture reagents were obtained from Sigma-Aldrich (St Louis, MO): 4-acetamidophenol, 1-aminobenzotriazole (ABT), bupropion (BUP), hydroxy-bupropion (OH-BUP), dextromethorphan (DEX), dextrorphan (DOR), dextrorphan glucuronide (DOR-glu), 3-methoxymorphinan (MOM), ketoconazole, quinidine, midazolam (MDZ), 1′-hydroxy-midazolam (1′-OH-MDZ), phenacetin (PHE), tolbutamide (TLB), 4-hydroxy-tolbutamide (4-OH-TLB), dimethylsulfoxide (DMSO), transferrin, linoleic acid, ascorbic acid, insulin, L-arginine and glucagon. The 1′-hydroxymidazolam glucuronide (1′-OH-Glu) was synthesized by the Isotope Chemistry and Metabolite Synthesis Department of Sanofi (Chilly-Mazarin, France).

Ham F12 and Williams E media, L-glutamine, HEPES, sodium pyruvate, penicillin, and streptomycin were purchased from Gibco (Paisley, UK). Long-term medium LDMM-A was obtained from In Vitro ADMET laboratories (Columbia, MD). The other chemicals and solvents used were all of analytical grade.

Human hepatocytes

Cryopreserved human hepatocytes were obtained from different providers (BD295 and BD304 from BD Gentest, Bedford, MA, and QHu4019 from Quest Pharmaceutical Services, Newark, DE). Available demographic information for patients including gender and age are reported in Supplementary Table 1 (Table S1).

LiverChip™ plate

The LiverChip™ design, as well as the key features and functionality have been described previously (Dash et al., 2009). Briefly, the LiverChip™ contains 12 ''bioreactors'', each comprising a culture well containing a collagen-coated scaffold, the dimension of which is engineered to recapitulate the capillary bed structure of the liver sinusoid, a micropump and a reservoir. Cell culture medium is passed through the scaffold/tissues via a pneumatically driven recycling perfusion mechanism. Each bioreactor is isolated from the others within the plate to provide twelve individually addressable wells for multi-sample testing (Figure 1).

Table 1. Reference substrates and specific enzymatic reactions catalyzed by the five main human CYP isoforms.

CYP	Marker substrate	Enzymatic reaction	Specific metabolite(s) quantified
CYP1A2	Phenacetin	O-deethylation	4-Acetamidophenol
CYP2B6	Bupropion	Methyl-hydroxylation	4-Hydroxy-bupropion
CYP2C9	Tolbutamide	Methyl-hydroxylation	4-Hydroxy-tolbutamide
CYP2D6	Dextromethorphan	O-Demethylation followed by conjugation	Dextrorphan (DOR) and DOR glucuronide (DOR-Glu)
CYP3A	Midazolam	1′-Hydroxylation followed by conjugation	1′-Hydroxy-midazolam (1′-OH-MDZ) and 1′-OH-MDZ-glucuronide (1′-OH-Glu)

Cell culture

Human hepatocyte preparation

Cryopreserved human hepatocytes were removed from liquid nitrogen and quickly thawed in a water bath at 37 °C. Human hepatocytes were transferred to a 50 mL-conical tube containing 40 mL pre-warmed BD Gentest™ (for BD295 and BD304) or CHRM™ (for QHu4019) cryohepatocyte recovery media and centrifuged at 100 × *g* (Jouan, GR4i) for 10 min at room temperature. After removing the supernatant, the cells were re-suspended in 2 mL of seeding medium. The seeding medium is a chemical medium adapted from Isom & Georgoff (1984), consisting of a 50/50 (v/v) mixture of Ham's F-12/William's E media supplemented with 10% v/v decomplemented fetal calf serum, insulin 10 µg/mL, 0.8 µg/mL glucagon, penicillin 100 UI/mL and streptomycin 100 µg/mL. Viability for the three human hepatocyte preparations was greater than 85% as measured by trypan blue exclusion. Cell concentration was adjusted to the desired inoculated cell density.

2D-static culture in 24-well microplates

Human hepatocytes suspended in the seeding medium were inoculated at 0.84×10^6 cells/mL into BD Biocoat™ collagen I 24-well microplates (BD Biosciences, Bedford, MA) in a final volume of 0.5 mL, i.e. corresponding to 0.42×10^6 cells/well. After 4 to 6 hours at 37 °C in a 5% CO_2 and 100% humidified atmosphere, period during which hepatocytes attached to the collagen-matrix, the plating medium was removed and replaced by the same serum-free culture medium (200 µL) supplemented with HEPES (3.6 g/L), ethanolamine (4 mg/L), transferrin (10 mg/L), linoleic acid-albumin (1.4 mg/L), glucose (252 mg/L), sodium pyruvate (44 mg/L), ascorbic acid (50 mg/L), arginine (104 mg/L), and L-glutamine (0.7 g/L). The following day, human hepatocytes were incubated with FDA-recommended metabolic CYP probe substrates (Table 1) at a starting concentration of 5 µM for midazolam, phenacetin and tolbutamide, 20 µM for dextromethorphan and 100 µM for bupropion, in 1.4 mL of 0.1% BSA (v/v)-containing incubation medium in the presence or in the absence of specific CYP inhibitors (1 µM furafylline for CYP1A2, 10 µM sulfaphenazole for CYP2C9, 3 µM quinidine for CYP2D6 and 3 µM ketoconazole for CYP3A) or total and not specific CYPs inhibitor (1 mM 1-aminobenzotriazole). The final solvent (DMSO) concentration never exceeded 0.2% (v/v). Fifty µL-supernatant aliquots (i.e. corresponding to the extracellular compartment) were taken at pre-determined times (0, 1, 2, 4, 6 and 24 h) and added to 350 µL of a mixture of acetonitrile/water (40/30 v/v). Samples were stored at −20 °C until analyzed by LC/MS-MS.

Dynamic culture in the LiverChip™ system

Human hepatocytes suspended in the seeding medium were inoculated into LiverChip™ plates at 0.6×10^6 cells/well in a final volume of 1.4 mL. Hepatocytes were allowed to attach on the scaffold in a 5% CO_2-incubator at 37 °C for 8 h thanks to a down flow at 1 µL/second. After hepatocyte adhesion, the medium was allowed to flow up from below the scaffold through the scaffold. The following day, the medium was renewed with 1.4 mL of long-term culture medium. After 3 additional days of culture, hepatocytes were incubated with FDA-recommended CYP probe substrates under experimental conditions identical to those described above for 2D-static conditions.

RNA isolation and gene expression analysis

Total RNA from human hepatocytes was extracted using RNeasy® 96 BioRobot 8000 kit Qiagen (Valencia, CA) according to instructions provided by the manufacturer. Reverse transcription (RT) was performed with 200 ng of isolated RNA using the High-Capacity cDNA Reverse Transcription Kit (Applied Biosystems, Foster City, CA). PCR was initiated using 50 µL Taqman® gene expression Master Mix (Applied Biosystems, Foster City, CA) and 50 µL of cDNA (30–1000 ng), on Applied Biosystem 7900HT Fast Real Time PCR in Taqman® Low-Density Array (TLDA) cards (Applied Biosystems, Foster City, CA). TaqMan Arrays' 384-wells were pre-loaded with gene specific primer/probe sets (listed in Supplementary Table S2). The Ct values of the target genes were normalized to 18 s rRNA and relative expression of target genes were determined by the ΔΔCt method as previously described (Livak & Schmittgen, 2001).

LC-MS/MS analysis for drug and metabolite quantification

Cell supernatants were analyzed for unchanged drug and specific metabolites (Table 1) by LC/MS-MS: phenacetin and 4-acetamidophenol for CYP1A2, tolbutamide and 4-hydroxy-tolbutamide for CYP2C9, bupropion and hydroxyl-bupropion for CYP2B6, dextromethorphan, dextrorphan and dextrorphan-glucuronide for CYP2D6, Midazolam, 1′-hydroxymidazolam and 1′-hydroxymidazolam-glucuronide for CYP3A activity. The data were collected and processed using MassLynx 4.1 Software from Waters-Micromass (Manchester, UK). The chromatograph (Acquity UPLC

system I Class) was fitted with an Acquity UPLC BEH C18 column (2.1 mm i.d. × 100 mm length, 1.7 µm particle size), coupled to a Xevo TQS mass spectrometer (all from Waters, Milford, MA) and used in electrospray ion positive mode except for tolbutamide and its hydroxyl metabolite which were analyzed in ion negative mode.

The mobile phase was a mixture of 1.5 g/L ammonium acetate–2 mL/L formic acid (solvent A) and acetonitrile 80%-methanol 20%–0.15 g/L ammonium acetate–formic acid 2 mL/L (solvent B). The solvent programmer was set to deliver a flow rate of 0.35 mL/min. Compounds were eluted in two minutes with a linear gradient from 10% to 100% solvent B over 1 min, followed by an isocratic step at 100% for 0.7 additional minute.

LC-MS/MS analysis for metabolites identification

Midazolam, dextromethorphan, bupropion, phenacetin, tolbutamide and their respective phase I and phase II metabolites were analyzed using a ThermoFisher Scientific Instruments (Waltham, MA) Accela LC system which consisted of a degasser, a quaternary pump and an HTC PAL autosampler (CTC Analytics) coupled to a Finnigan LTQ-Orbitrap instrument (San Jose, CA) with an ESI source and HCD collision cell. The separation was performed on an YMC-pack J'sphere H80 (Dinslaken, Germany) (250 mm × 2.1 mm, i.d., 4 µm) column and the column temperature was set at 38 °C. Gradient elution was performed with a 5 mM aqueous ammonium acetate buffer containing 0.1% (v/v) formic acid as mobile phase A, and acetonitrile as mobile phase B. The flow rate was 350 µL/min. Separation of metabolic probes from their metabolites was achieved by optimizing the phase-B elution gradient. Injection volume was set at 25 µL.

The MS conditions employed are as follows: positive and/or negative scan modes from *m/z* 100 to 1000 (full scan mass spectrum at a resolution of 30 000); sheath gas, nitrogen at a flow rate of 30 arbitrary units (AU); auxiliary gas, nitrogen at flow rate of 15 AU; spray voltage, 5.00 kV; ion transfer capillary temperature, 250 °C; maximum injection time, 500 ms; HCD at 35 eV (MS/MS, positive scan mode).

The instrument was mass calibrated prior to the analysis by infusing a Positive Mode Cal Mix provided by Supelco at a flow rate of 5 µL/min, using a syringe pump.

SEM and TEM microscopy

Seven days after seeding hepatocytes in the LiverChip™ (Oxfordshire, UK) device, selected scaffolds from human hepatocyte batch QHu4019 were fixed in 2% glutaraldehyde for at least 24 hours, rinsed 3 times with 0.1 M cacodylate buffer pH 7.2, impregnated with 1% osmium tetroxide (OsO_4, Sigma-Aldrich, St Louis, MO) for 2 h, then dehydrated in solutions of alcohol at increasing concentrations (30°, 50°, 70°, 80°, and 90° for 15 min per concentration, then 100° for one night). For TEM examination, the dehydrated samples of the scaffolds were embedded in an epoxy resin (EMbed 812, EPON TM), scaffold samples being oriented parallel and perpendicular to the plane of future section of the resin blocks; after polymerization (2 days at 60 °C), blocks were sectioned at 500 Å with a Leica Ultracut UCT ultra-microtome (Wetzlar, Germany), sections were laid on 200 mesh copper grids and examined with a Jeol 1010 TEM at 80 kV. For SEM, the dehydrated scaffold samples were subjected to critical point drying (Leica EM CPD300), metallized with 300–500 Å gold particles, and examined with a Jeol 6060LV SEM (Peabody, MA). TEM pictures were obtained with a MegaView III (Olympus, Tokyo, Japan) digital camera.

Fluorescence microscopy

Viability of hepatocytes in the Liverchip™ device was qualitatively assessed by using live (Calcein-AM, Invitrogen, Carlsbad, NM), dead (ethidiumhomodimer-1, Invitrogen) and general nuclei staining (Hoechst 33342, Lonza, Bâle, Switzerland) markers. FITC anti- human albumin antibody was used to stain synthesized albumin (Rockland, Gilbertsville, PA). Fluorescence microscopy was performed using a LSM 510 Meta confocal microscope (Carl Zeiss).

Hepatocyte functional assay

The daily albumin production was measured using human albumin enzyme-linked immune-sorbent assay quantitation kit (Bethyl laboratories Inc., Montgomery, TX). Functional data were normalized to 10^6 cells based on the number of seeded cells.

Data analysis

Calculation of intrinsic clearance

In human hepatocytes, the intrinsic *in vitro* metabolic clearance (Cl_{int}) was calculated using WinNonLin (St Louis, MO) PK analysis software version 5.2. Unchanged drug disappearance kinetics data were fitted to a first-order elimination equation:

$$C = C_0 \cdot e^{-k_e \cdot Vt}$$

where C is the measured concentration at any time, C_0 is the concentration at zero-time and k_e is the elimination constant. The decrease in substrate was exponential over time for all reported Cl_{int} values. Curve fitting was performed after natural logarithm transformation of the concentration data.

Intrinsic clearance was calculated as follows:

$$Cl_{\text{int}}\left(\text{mL/h}/10^6\,\text{cells}\right) = k_e \cdot V$$

where V is the incubation volume expressed in mL normalized to 10^6 hepatocytes.

Results

Morphological and functional behavior of cells in the dynamic LiverChip™ system

Hepatocyte morphology and microtissue formation after the cell adhesion phase (4 h post-seeding) and at the end of each experiment (Day 7) are presented in Figure 2. Optical microscopy images showed that the cellular structures formed during the two first days in culture remained stable during this culture period. A live/dead fluorescent stain indicated that liver cells exhibited a high viability with only a few dead cells observed in the perfused multiwell system after seven days of culture (Figure 3). To evaluate hepatocyte function, scaffolds were stained with conjugated albumin-fluorescein. Retention of this hepatocyte-specific functional marker (Figure 4B) over the period of culture was confirmed

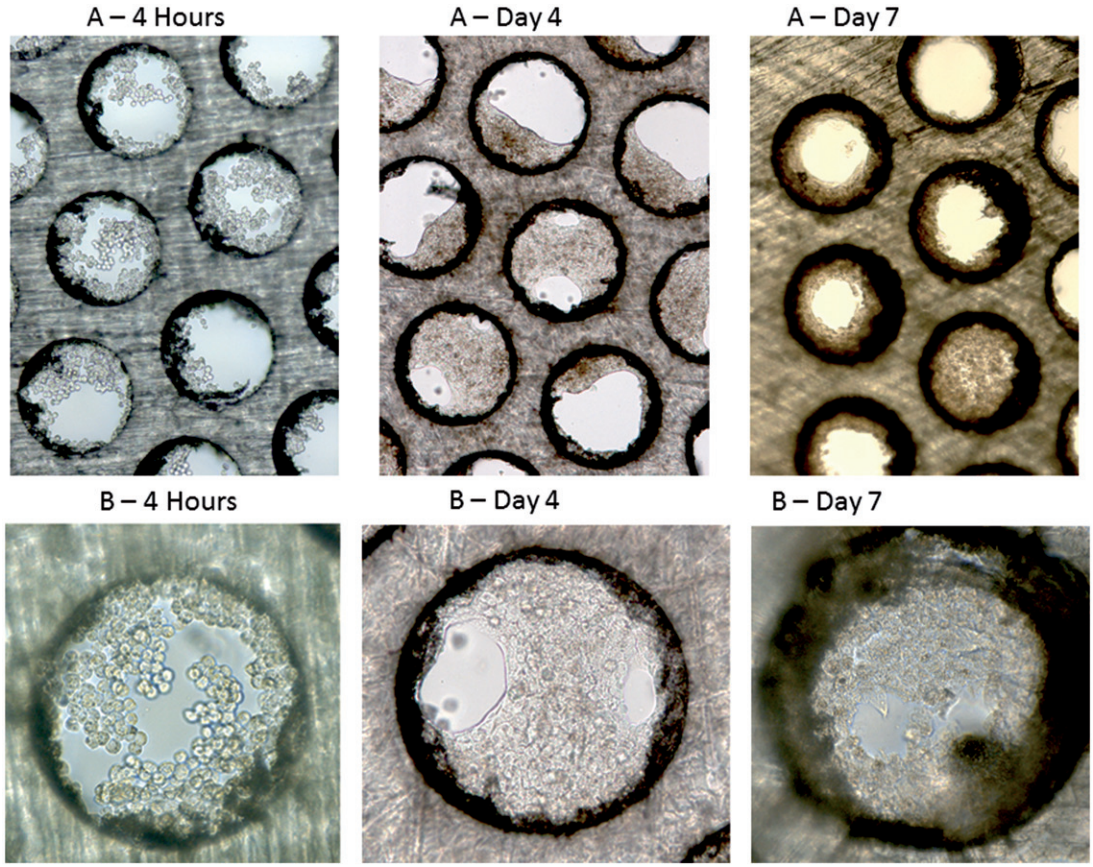

Figure 2. Optical microscopy: morphogenesis of human hepatocytes from preparation QHu4019 in the LiverChip™ scaffold from 4 h to 7 days after seeding hepatocytes in the LiverChip™ device at (A) magnification ×10 and (B) magnification ×20.

Figure 3. Fluorescence microscopy: images of one channel in the scaffold populated with human hepatocytes from batch QHu4019 (A) after 7 days of culture. Nuclei were stained with Hoechst-33342 (B) and dead cells were detected by ethidium homodimer-1 (C), while viable cells were detected by calcein AM (D). Channel boundary is highlighted by a white dashed line. Bar = 100 µm.

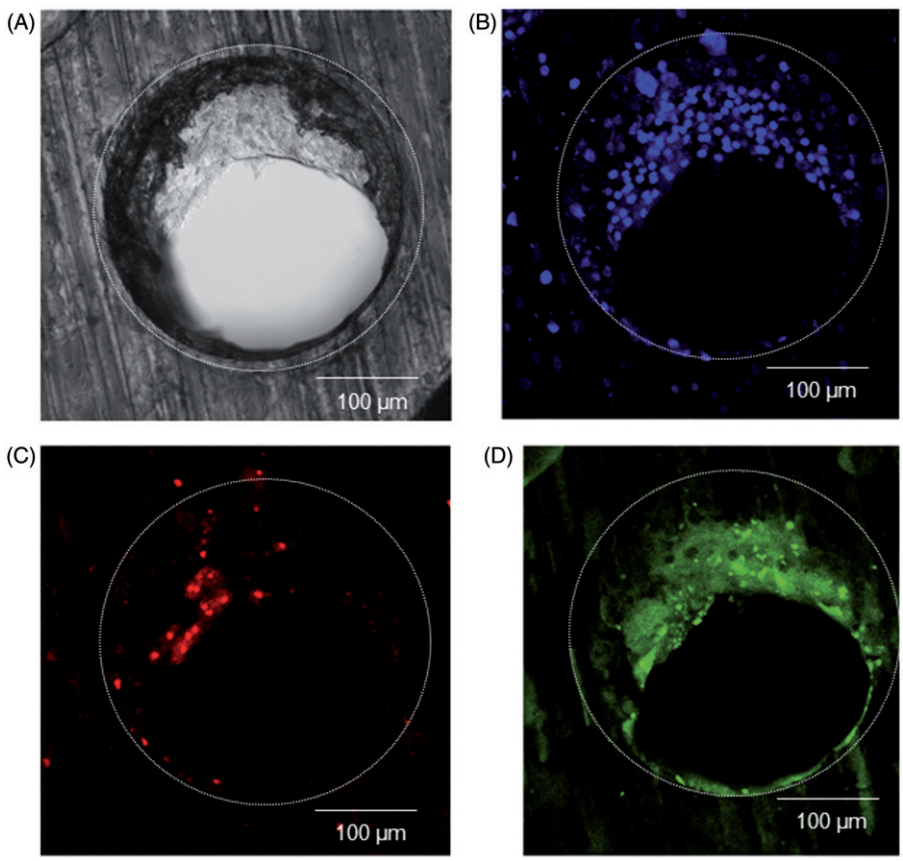

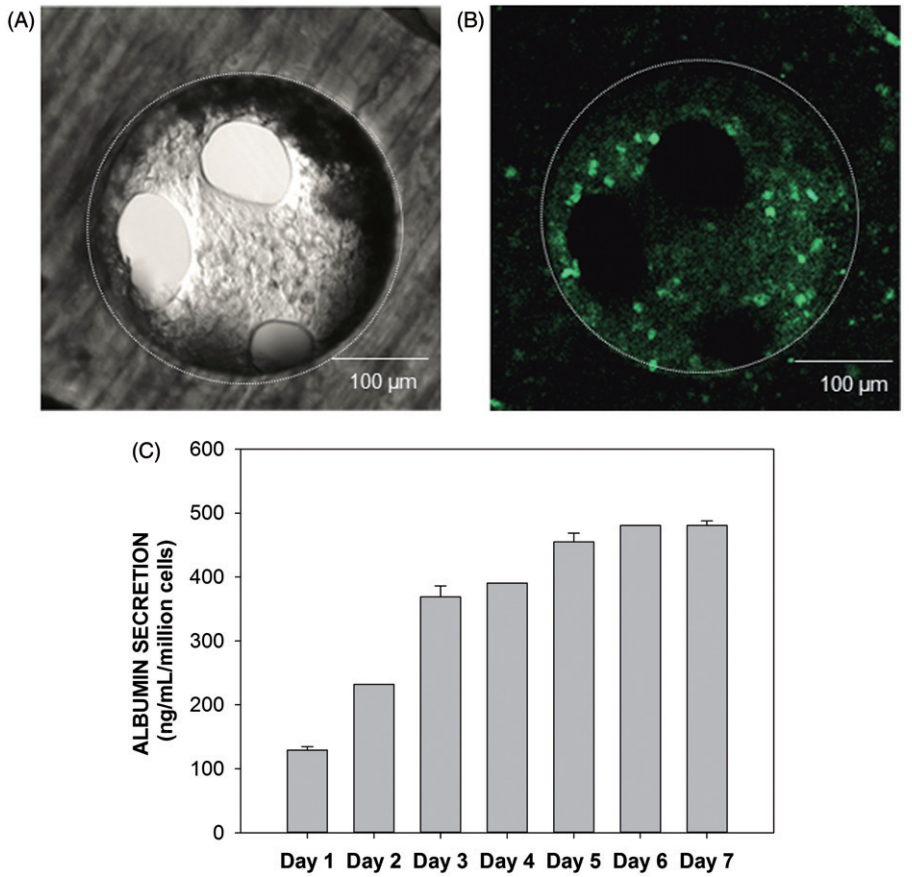

Figure 4. Functional maintenance of albumin secretion in human hepatocytes (QHu4019 batch) under dynamic LiverChip™ conditions: optical and fluorescence microscopy images of one channel obtained after 7 days of culture (A). Albumin was stained in green with human albumin antibody (B). Channel boundary is highlighted by a white dashed line (Bar = 100 mm). Human hepatocytes were cultured under dynamic LiverChip™ conditions over 7 days. Each day (one bar per day), the extracellular compartment was sampled and analyzed for albumin secretion (C).

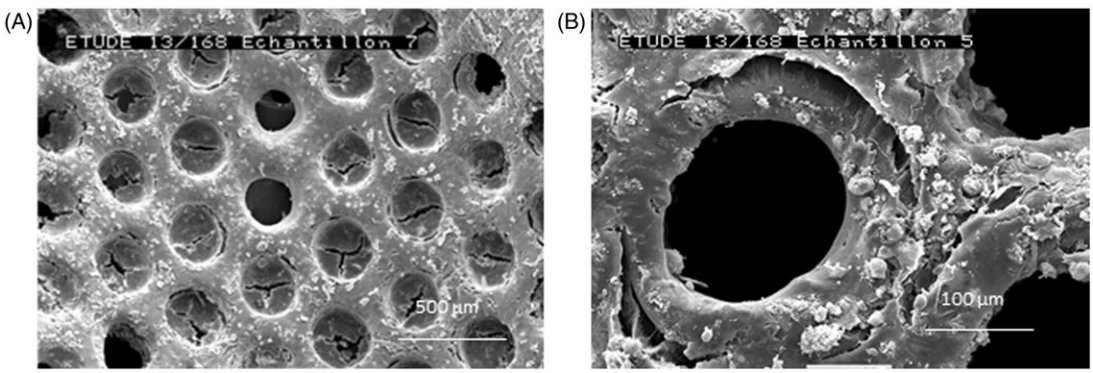

Figure 5. Scanning Electron Microscopy: LiverChip™ scaffolds after 7 days of culture with human hepatocytes from batch QHu4019. (A) Picture (×50) of a LiverChip™ scaffold, showing cell population (hepatocytes) covering the surface of the scaffold and populating the channels of the scaffold. Largely populated channels are totally filled with hepatocytes. (Bar = 500 µm) (B) Higher magnification (×200) of the LiverChip™ scaffold, showing the hepatocyte monolayer, approximately 80–100 µm thick, within a few channels of the scaffold, with cellular debris or necrotic hepatocytes expelled to the surface of cells (NB: cracks at the limit of the channels reflect drying artifacts during critical point drying process). Bar = 100 µm.

by measurement of albumin secretion (Figure 4C). Scanning electron microscopy analysis (Figure 5) showed that the hepatocyte population uniformly covered the wall of the scaffold channels, as well as the surface of the scaffold. The hepatocytes occasionally penetrated into the scaffold channels. Debris of necrotic cells mixed with bile elements were noted at the surface of the cells, in the form of small round structures. TEM analysis (Figure 6) of the *in vitro* hepatocytes revealed morphological and ultra-structural features that are typically observed in viable hepatocytes *in vivo*: bile canaliculi with microvilli and cell junctions, abundant mitochondria, rough endoplasmic reticulum, glycogen storage and a few lipid globules. These characteristic features indicated that hepatocellular structure and metabolic function were maintained under the conditions of the microfluidic LiverChip™ system.

Gene expression

Basal mRNA expression of the main cytochrome – P450's (CYP's) in the dynamic LiverChip™ system

The relative mRNA expression of the main CYP's involved in drug metabolism, i.e. CYP1A2, CYP2B6, CYP2C8, CYP2C9, CYP2C19, CYP2D6 and CYP3A4, was analyzed in dynamic

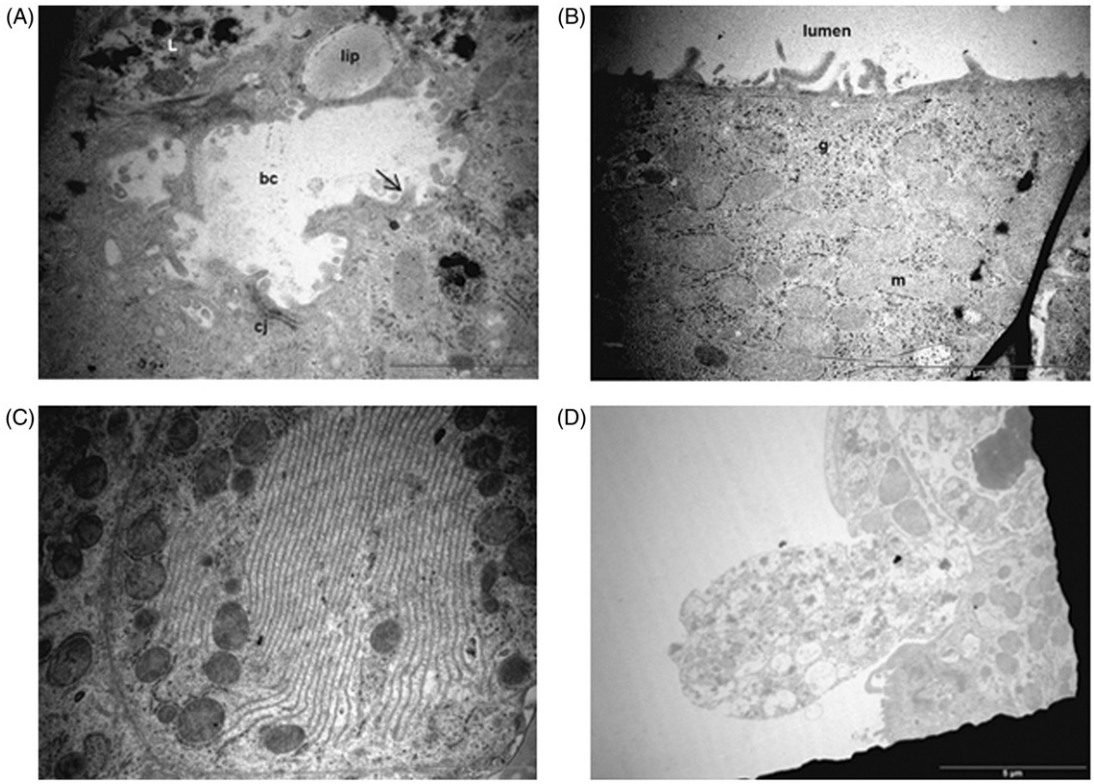

Figure 6. TEM: ultrastructural analysis of human hepatocytes from batch QHu4019 maintained in the perfused multiwell system for 7 days. (A) Large bile canaliculi (bc) at the junction of several hepatocytes, with their typical limiting cell junctions (cj) and microvilli (arrows). Occasional lipid inclusions (lip) are also observed. (Bar = 2 μm). (B) Abundant mitochondria (m), glycogen storage structures (g), and formation of small microvilli at the luminal surface. (Bar = 5 μm). (C) Many hepatocytes exhibited rough endoplasmic reticulum (RER) expression, occasionally forming stacks of RER. (Bar = 2 μm). (D) Necrotic hepatocytes at the luminal surface represent expelled hepatocytes (corresponding to debris/necrotic cells seen by SEM [see Figure 5B] and to dead cells observed with ethidium homodimer-1 stain [see Figure 3C]) (Bar = 5 μm).

LiverChip™ conditions from Day 1 to Day 7 post-cell thawing, in 3 cryopreserved human hepatocyte preparations (Figure 7A). As the mRNA profiles were relatively different from one donor to another, standard deviations of the mean values were not determined. Hence, only mRNA gene expression tendencies during the incubation period are discussed. The viability of hepatocytes and associated basal expression of the main *CYP* genes were maintained from Day 1 to Day 7 under the dynamic LiverChip™ conditions as measured by LDH release (data not shown). Basal expression of the *CYP2B6* gene was consistently up-regulated during the 7 days of the experiments. Basal mRNA expression of *CYP1A2*, *CYP2C19* and *CYP3A4* genes was unchanged or slightly down-regulated while the basal expression of the *CYP2C8*, *CYP2C9* and *CYP2D6* genes was down-regulated during the same 7 day period.

Basal mRNA expression of the main phase II enzymes in the dynamic LiverChip™ system

To evaluate cell functionality, RTqPCR analysis was also performed on the genes of four phase II enzymes, i.e. *UGT1A1*, *UGT1A6*, *UGT2B7* and *UGT2B17*, over a 7-day period (Figure 7B). Except for Day 1, the levels of the genes of the 4 phase II UGT enzymes remained unchanged or were up-regulated during the 7-day period of culture.

Basal mRNA expression of the main transporters in the dynamic LiverChip™ system

RTqPCR analysis of the mRNA expression levels of transporter genes was also performed in untreated hepatocyte cultures during the 7-day culture period (Figure 7C). The levels of the genes related to most of the uptake transporters (*OCT1*, *NTCP*, *OATP1B1* and *OATP2B1*) were partially recovered after 1 Day of culture, except for the *OATP1B3* gene for which the expression level was dramatically reduced. Genes of the efflux transporters were either mostly maintained or slightly/moderately up-regulated (*BCRP*, *MRP2*, *MDR1*) over the 7-day period except for the *BSEP* gene which was down-regulated.

Basal mRNA expression of the nuclear receptor genes in the dynamic LiverChip™ system

RTqPCR analysis of the mRNA expression levels of the nuclear receptor genes, i.e. *PXR* and *CAR* genes, in untreated cultures of human hepatocytes during the 7-day period (Figure 7B) showed that the levels of the two analyzed nuclear receptor genes were maintained unchanged or slightly down-regulated over time.

Metabolism analysis

To evaluate the metabolic activities of cryopreserved human hepatocytes in dynamic LiverChip™ system in comparison to

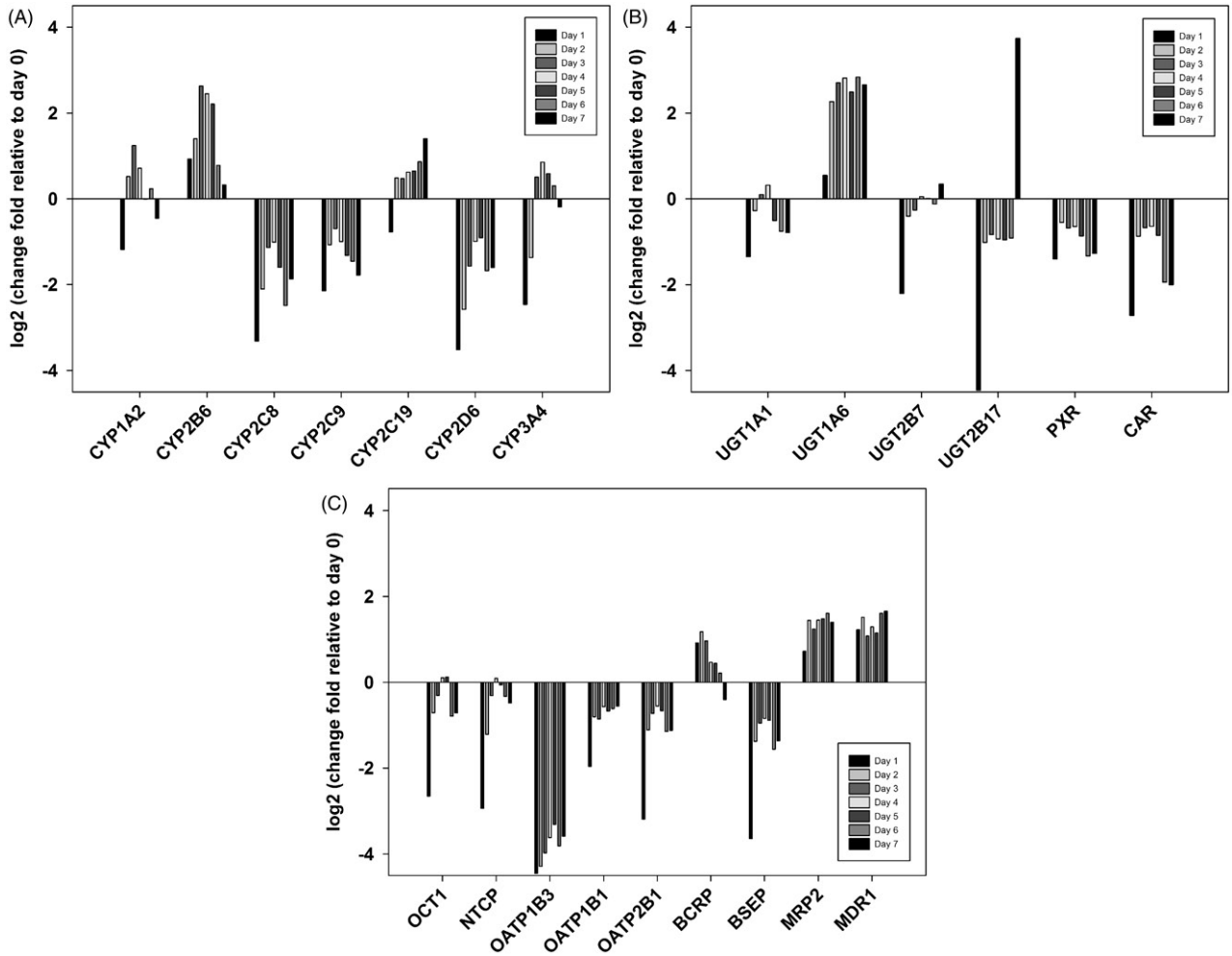

Figure 7. Enzyme, transporter and nuclear receptor gene expression analysis: effects of culture duration on gene expression levels of phase I enzymes (A), phase II enzymes (B), nuclear receptors (B) and transporters (C) in cryopreserved human hepatocytes (mean of three different human hepatocyte preparations, i.e. QHu4019, BD304 and BD295) in the dynamic LiverChip™ system. Constitutive expression of genes is expressed as log two-fold changes relative to Day 0, post-thawing. Expression levels were normalized to 18 s RNA levels, which were invariant per cell across the different incubation times. Data obtained from $n = 2$ for each point. Genes are classified as unchanged for log 2-fold changes in the range -1 to $+1$; slightly down-regulated for log 2-fold changes in the range -1 to -2; moderately down-regulated for log 2-fold changes in the range -2 to -4, and strongly down-regulated for log 2-fold changes in the range -4 to $-\infty$, with a similar semantic convention for up-regulated genes.

2D-static conditions, metabolism of five probes representative of main CYPs was investigated (Table 1). In the case of 2D-static conditions, experiments were performed at Day 1 after cells seeding, i.e. conditions under which enzyme/metabolic activity is the highest before global dedifferentiation process occurred, while for dynamic LiverChip™ conditions, metabolic studies were run at Day 4, when micro-tissues were well formed and hepatocytes exhibited a well differentiated and functional phenotype.

Non-specific binding

Before characterizing CYPs activities of human hepatocytes in the LiverChip™ system, preliminary studies have been performed in order to investigate the non-specific binding of the five probe substrates on the device. The 5 molecules circulated in the perfusion circuit and 3D scaffold without cells for 24 h, and the ratio of each substrate was calculated to the initial concentration. After 24 h incubation time, less than 20% of each compound was bound on the 3D-dynamic LiverChip™ device.

Evaluation of CYP1A2 activity of cryopreserved human hepatocytes in the dynamic conditions of the LiverChip™ system in comparison to 2D-static conditions

Following a 24-hour incubation of 5 µM phenacetin with human hepatocytes under 2D-static conditions, phenacetin disappearance was associated with the formation of one major metabolite, identified as 4-acetamidophenol. When the same substrate was incubated under dynamic LiverChip™ conditions on Day 4, a similar LC/MS-MS spectrum was observed except that the percentage of 4-acetamidophenol formed was much higher in comparison to that observed under 2D-Static conditions, suggesting a higher CYP1A2 metabolic capacity under dynamic conditions (LC/MS-MS spectrum not shown). LC/MS-MS quantification of phenacetin and its major metabolite over the 24-hour incubation period (Figure 8A1 and B1) confirmed the observations of the metabolite identification analyses. Indeed, 8.5% of phenacetin was biotransformed to 4-acetamidophenol during the first 24 h of incubation in the 2D static system, while, under dynamic LiverChip™ conditions, the biotransformation was close to

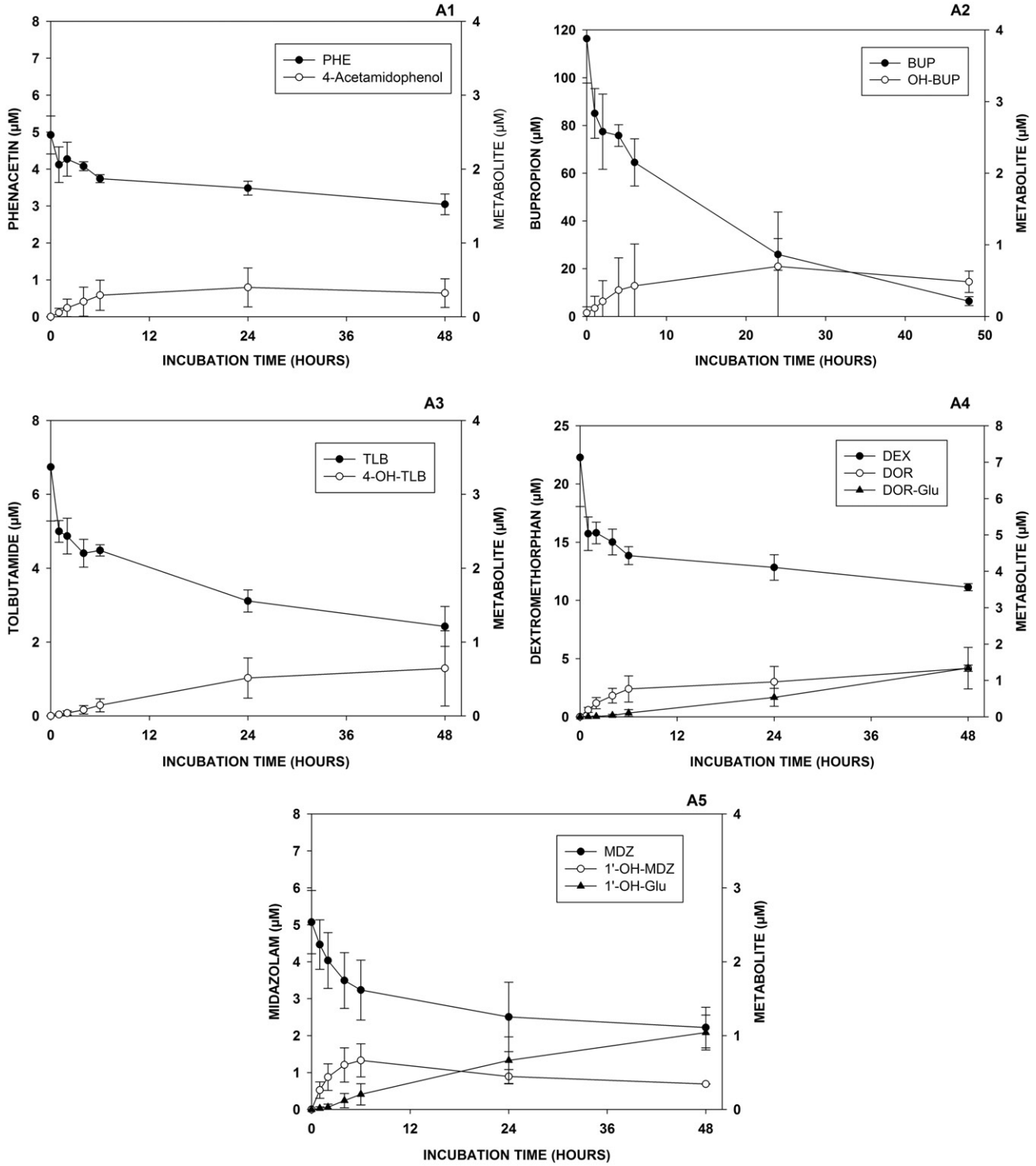

Figure 8. Kinetics of the metabolism of probe substrates of the major CYP isoforms, i.e. phenacetin, bupropion, tolbutamide, dextromethorphan and midazolam, in both 2D-static conditions (A1 to A5) and under dynamic conditions in the LiverChip™ (B1 to B5). Results are expressed as the mean of 3 donors, each donor being the mean of at least duplicates.

36% (Table 2). Higher CYP1A2 activity in dynamic LiverChip™ conditions was also observed when evaluating the *in vitro* intrinsic clearance of phenacetin on Day 4 post-seeding as the rate of phenacetin disappearance (Table 3) was 7-fold higher than that determined under 2D-static conditions (0.277 mL/h/10^6 cells and 0.038 mL/h/10^6 cells, respectively).

When incubated in the presence of furafylline, a specific CYP1A2 inhibitor, the formation of 4-acetamidophenol was completely abolished as observed in 2D-static conditions (data not shown).

Evaluation of CYP2B6 activity of cryopreserved human hepatocytes in the dynamic conditions of the LiverChip™ system in comparison to 2D-static conditions

Following incubation of 100 µM bupropion with human hepatocytes under 2D-static conditions, bupropion

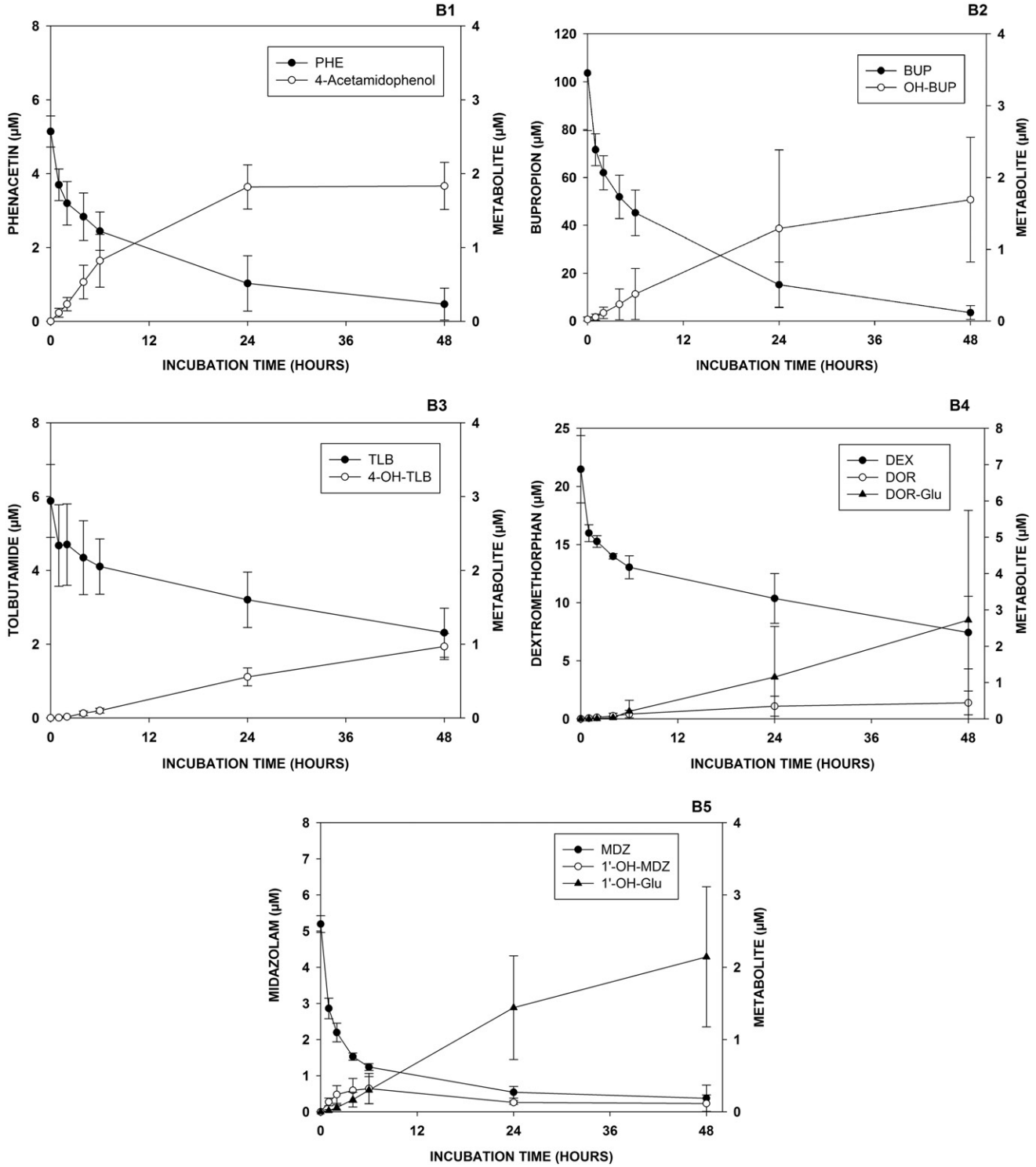

Figure 8. Continued.

disappearance was associated with the formation of two metabolites, a major one identified as an alcoholic derivative and a minor one identified as the specific CYP2B6-dependent hydroxyl metabolite (Faucette et al., 2000; Hesse et al., 2000) (Supplementary Figure S1). When incubated under dynamic LiverChip^{TM} conditions on Day 4, a similar metabolic profile was observed with a slight higher percentage of hydroxy-bupropion formed in comparison to that determined under 2D-Static conditions (Figure 8A2 and B2). This suggests that CYP2B6 metabolic capacity was higher under dynamic conditions used in the LiverChip^{TM} system. This was confirmed in the experiments of intrinsic clearance determination in which a 1.3-fold greater mean intrinsic clearance was observed under dynamic conditions (Table 3), while the percentage of hydroxy-bupropion formed after 24 h incubation was 1.9-fold greater in the LiverChip^{TM} system (Table 2). In the presence of ABT, the formation of the specific CYP2B6 metabolite, hydroxy-bupropion from the probe substrate buproprion was completely abolished, which is consistent with ABT being a total CYP inhibitor while it had

Table 2. Specific CYP-mediated metabolite formation.

	Phenacetin		Bupropion		Tolbutamide		Dextromethorphan		Midazolam	
Condition	Static	Dynamic	Static	Dynamic	Static	Dynamic	Static	Dynamic	Static	Dynamic
BD295	8.4	43.8	0.2	2.3	4.0	9.7	9.9	15.1	13.8	44.6
BD304	14.5	30.2	1.6	1.2	9.8	8.6	4.3	2.1	34.8	14.4
QHu4019	2.5	32.7	0.2	0.3	7.9	10.1	6.2	4.9	20.7	32.6
Mean	8.5	35.6	0.7	1.3	7.2	9.5	6.8	7.4	23.1	30.5
SD	6.0	7.2	0.8	1.0	2.9	0.8	2.9	6.8	10.7	15.2
Fold increase*	4.2		1.9		1.3		1.1		1.3	

Results are expressed as the mean of the percentage biotransformation of CYP probe substrate after 24 h incubation, derived from the concentration of the probe substrate after 24 h relative to the initial probe concentration at T_0 for 3 donors (% biotransformation was determined in duplicate, at least, for each of the 3 donor preparations).
*Fold-increase = ratio of mean % biotransformation under dynamic conditions compared to mean % biotransformation under static conditions.

Table 3. *In vitro* intrinsic clearance calculated from unchanged drug disappearance.

	Phenacetin		Bupropion		Tolbutamide		Dextromethorphan		Midazolam	
Condition	Static	Dynamic	Static	Dynamic	Static	Dynamic	Static	Dynamic	Static	Dynamic
BD295	0.050	0.368	0.210	0.449	0.047	0.042	0.063	0.125	0.069	0.649
BD304	0.034	0.105	0.160	0.114	0.121	0.086	0.042	0.036	0.169	0.908
QHu4019	0.030	0.357	0.479	0.567	0.069	0.040	0.067	0.078	0.101	0.760
Mean	0.038	0.277	0.283	0.377	0.079	0.056	0.033	0.079	0.113	0.772
SD	0.010	0.135	0.172	0.235	0.038	0.026	0.013	0.044	0.172	0.130
Fold increase*	7.3		1.3		0.7		2.4		6.4	

$Cl_{int,vitro}$ values are expressed in mL/h/10^6 cells. At least duplicate experiments were performed with each of the three hepatocyte donors. The Cl_{int} determinations were carried out as described under the section ''Material and Methods''.
*Fold-increase = ratio of mean Cl_{int} values under dynamic conditions compared to mean Clint values under static conditions.

no inhibitory effect on the formation of the alcoholic metabolite which is mediated by cytosolic enzymes (Meyer et al., 2013) (Supplementary Figure S1).

Evaluation of CYP2C9 activity of cryopreserved human hepatocytes under dynamic conditions in the LiverChip™ system in comparison to 2D-static conditions

Following incubation of 5 μM tolbutamide with human hepatocytes under dynamic LiverChip™ system conditions (only CYP2C9-dependent metabolism of the probe substrate) tolbutamide was observed, with the successive formation of the 4-hydroxyl and the carboxylic acid derivatives The formation of these two metabolites was completely abolished in the presence of sulphaphenazole, a specific and potent CYP2C9 inhibitor (Supplementary Figure S2). Similar metabolite production profiles were observed between dynamic and 2D-static conditions. Finally, the intrinsic clearance of tolbutamide (Table 3) and the formation of 4-hydroxy-tolbutamide (Table 2) were also similar under 2D-static and dynamic LiverChip™ conditions. This result is consistent with the metabolic capacity of CYP2C9 in human hepatocytes being similar under both, 2D-static conditions after one day of culture and dynamic conditions in the LiverChip™ system at Day 4 (Figure 8A3 and B3).

Evaluation of CYP2D6 activity of cryopreserved human hepatocytes under dynamic conitions in the LiverChip™ system in comparison to 2D-static conditions

The kinetics of dextromethorphan disappearance and formation of its major metabolites, dextrorphan, DOR and dextrorphan-glucuronide, DOR-Glu, in both 2D-static and dynamic LiverChip™ conditions, are presented in Figure 8A4 and B4. The rate of formation of the O-glucuronide of dextrorphan (i.e. DOR-Glu) was considerably higher under the dynamic conditions of the LiverChip™ system than under 2D-static conditions, indicating higher UGT2B activities under dynamic conditions (Lutz & Isoherranen, 2012). Furthermore, the *in vitro* intrinsic clearance of dextromethorphan (Table 3) and the formation of its major metabolites (Table 2) reflected the relatively higher CYP2D6 activity under the dynamic conditions of the LiverChip™ system compared to those under the 2D-static conditions.

Following incubation of 20 μM Dextromethorphan with human hepatocytes under dynamic LiverChip™ system conditions, numerous metabolic pathways were observed, which consisted of N-demethylation to yield the 3-methoxymorphinan (MOM), hydroxylation at different sites of the molecule to form hydroxyl metabolites. OH-DEX and O-demethylation to yield dextrorphan (DOR) followed by O-glucuronidation (DOR-Glu). When hepatocytes were incubated in the presence of quinidine, a specific and potent CYP2D6 inhibitor a substantial decrease in both dextrorphan and its glucuronide was observed, as expected (Takashima et al., 2005), while both N-demethylation and hydroxylation of the probe substrate were not affected. Conversely, when incubations were performed in the presence of ketoconazole, a specific and potent CYP3A inhibitor, almost complete suppression of the formation of the hydroxyl metabolite together with a decrease in MOM formation was observed. This was associated with an increase in the formation of dextrorphan and its glucuronide via the CYP2D6-dependent pathway. This increase may be

the consequence of a higher quantity of dextromethorphan substrate being available for CYP2D6-dependent metabolism when the CYP3A pathway was completely inhibited. All of these metabolic pathways were completely inhibited in the presence of ABT, a total CYP inhibitor (Supplementary Figure S3).

Evaluation of CYP3A activity of cryopreserved human hepatocytes under dynamic conditions in the LiverChip™ system in comparison to 2D-static conditions

The kinetics of midazolam disappearance and formation of its major metabolites (1′-OH-midazolam and 1′-OH-Midazolam-glucuronide) are presented in Figure 8A5 and B5. The percentage of biotransformation and hence metabolite formation was higher in the dynamic LiverChip™ system than in the 2D-static system. This was confirmed by comparison of the *in vitro* intrinsic clearance of midazolam under both dynamic and static conditions. Results showed that the mean intrinsic clearance was 6.4-fold greater under the dynamic conditions of the LiverChip™ system (Table 3). In addition, the percentage biotransformation of midazolam was 1.3-fold greater under dynamic conditions compared to 2D static conditions (Table 2), which is a reflection of the higher CYP3A and UGT2B4/7 enzyme activities in the dynamic LiverChip™ system.

Following incubation of 5 µM Midazolam with human hepatocytes (preparation BD295) under 2D-static conditions, midazolam disappearance was associated with the predominant formation of its 1′-hydroxyl metabolite, either under the aglycone form or conjugated with glucuronic acid, i.e. a CYP3A/UGT2B4/7-dependent pathway. In addition, other metabolites were also observed such as the 4-hydroxyl derivative and the direct N-glucuronides of midazolam which were specifically formed by UGT1A4 (Klieber et al., 2008) (Figure 9A). When incubated under dynamic LiverChip™ conditions on Day 4 or 2D static conditions after one day of culture, no major difference was noted in terms of the qualitative kinetics of biotransformation of midazolam behaviour, since the same metabolites were detected under both conditions. However, a marked difference in the quantitative aspects of biotransformation and metabolite formation was observed under the dynamic and static conditions, in particular in the CYP3A/UGT2B4/7-dependent pathways (Figure 9B). When incubated in the presence of ketoconazole, the decrease observed in the formation of both 1′-hydroxyl-midazolam and its glucuronide (1′-OH-Glu) compared to the level of these metabolites in the absence of

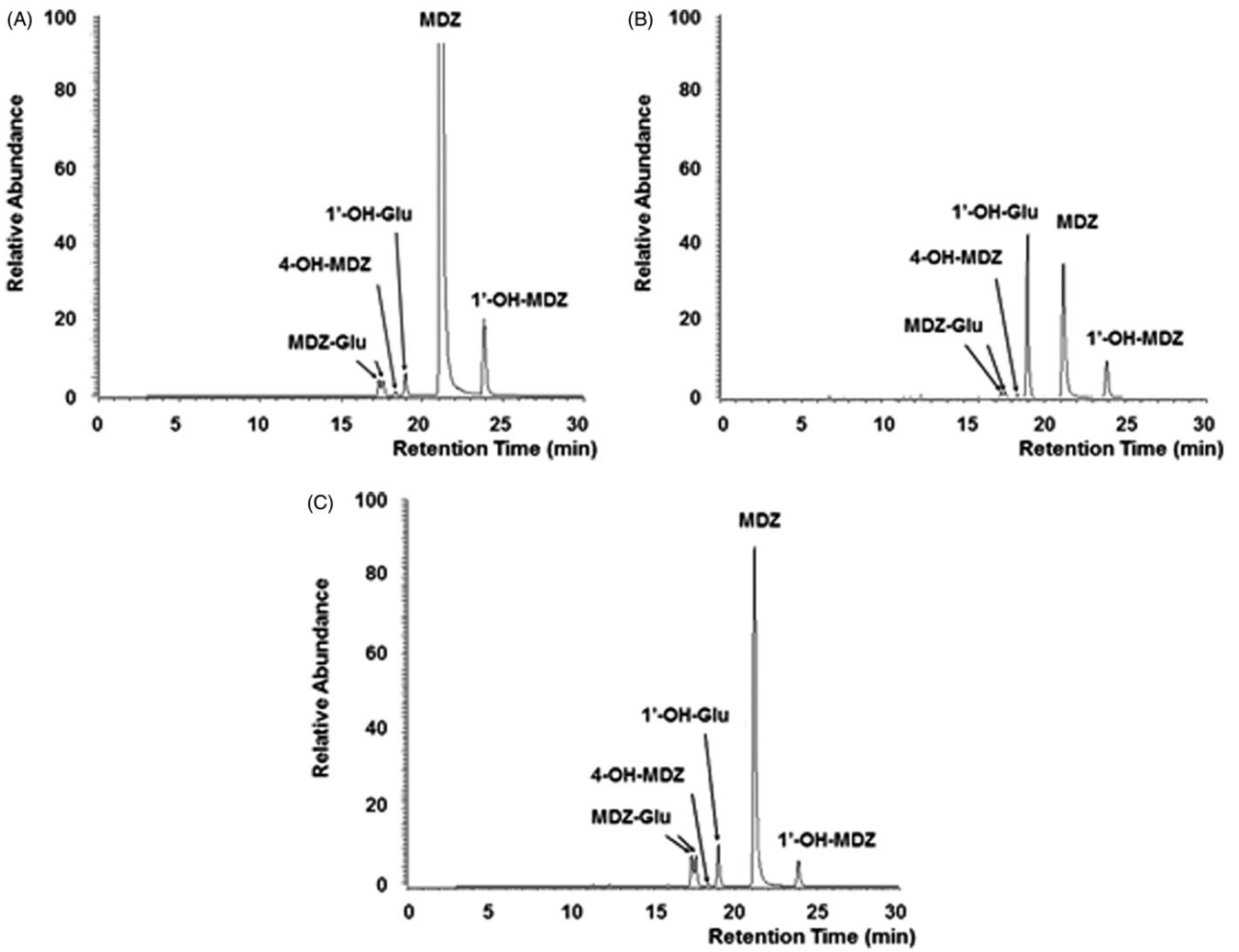

Figure 9. Mass spectrometry profiles obtained following a 24-hour incubation of human hepatocytes (preparation BD295) *in vitro* with 5 µM Midazolam, (A) in 2D-static conditions on Day 1, or in dynamic LiverChip™ conditions on Day 4 in the absence (B) or the presence of ketoconazole (C).

ketoconazole was associated with both an increase in the concentration of parent drug and the increased metabolism of midazolam through direct N-glucuronidation, which is catalyzed by UGT1A4 (Figure 9C). In dynamic conditions, kinetics of midazolam disappearance and metabolite formation, in the presence or absence of different CYP inhibitors (ketoconazole or ABT), were determined using the QHu4019 preparation (Figure 10). In the absence of inhibitor (Figure 10A), the disappearance of midazolam was mainly associated with the formation of 1′-hydroxyl-midazolam and its glucuronide although additional minor metabolites such as midazolam N-glucuronides and 4-hydroxy-midazolam, were also observed. When incubated with ketoconazole (Figure 10B), the specific CYP3A inhibitor, a minor increase in the concentration of unchanged midazolam was observed. This was associated with a marked decrease in the formation of both 1′-hydroxy-midazolam and its glucuronide. Over the 6–24-hour period of incubation, a recovery of the formation of midazolam metabolites was noted. This was due to a lack of ketoconazole in the incubation medium, this latter being extensively metabolized during the initial 0–6-hour-period. Indeed, more than 90% of ketoconazole was metabolized through two major metabolic pathways, loss of the acetaldehyde moiety and piperazine oxidation (data not shown). As expected, in the presence of ABT (Figure 10C), a complete abolishment of all CYP-dependent metabolites formation was observed.

To evaluate the maintenance of metabolic activity of human hepatocytes in the dynamic LiverChip^{TM} system as a function of culture time, the kinetics of midazolam disappearance and metabolite formation (1′-hydroxyl-midazolam: 1′-OH-MDZ and 1′-hydroxy-midazolam glucuronide: 1′-OH-Glu) were investigated 4 and 7 Days after cells adhesion in one cryopreserved human hepatocyte preparation (BD295). The kinetics of the disappearance of unchanged drug and metabolite formation on Day 4 and Day 7 post-seeding were similar. Whatever the day of culture, midazolam was extensively metabolized with more than 75% of the initial drug concentration being metabolized after a 6-hour incubation. After 24 h incubation, approximately 90% of midazolam has been metabolized and the total of the extracellular concentration, of both CYP3A-dependent metabolites, ‘‘1′-OH-MDZ and 1′-OH–Glu’’ represented 40–50% of the initial midazolam concentration. The intrinsic metabolic clearance of midazolam confirmed that CYP3A-dependent metabolic capacity was similar on Days 4 and 7 ($CL_{int\ Day\ 4} = 1.04$ mL/h/10^6 cells versus $CL_{int\ Day\ 7} = 1.28$ mL/h/10^6 cells; $n = 1$).

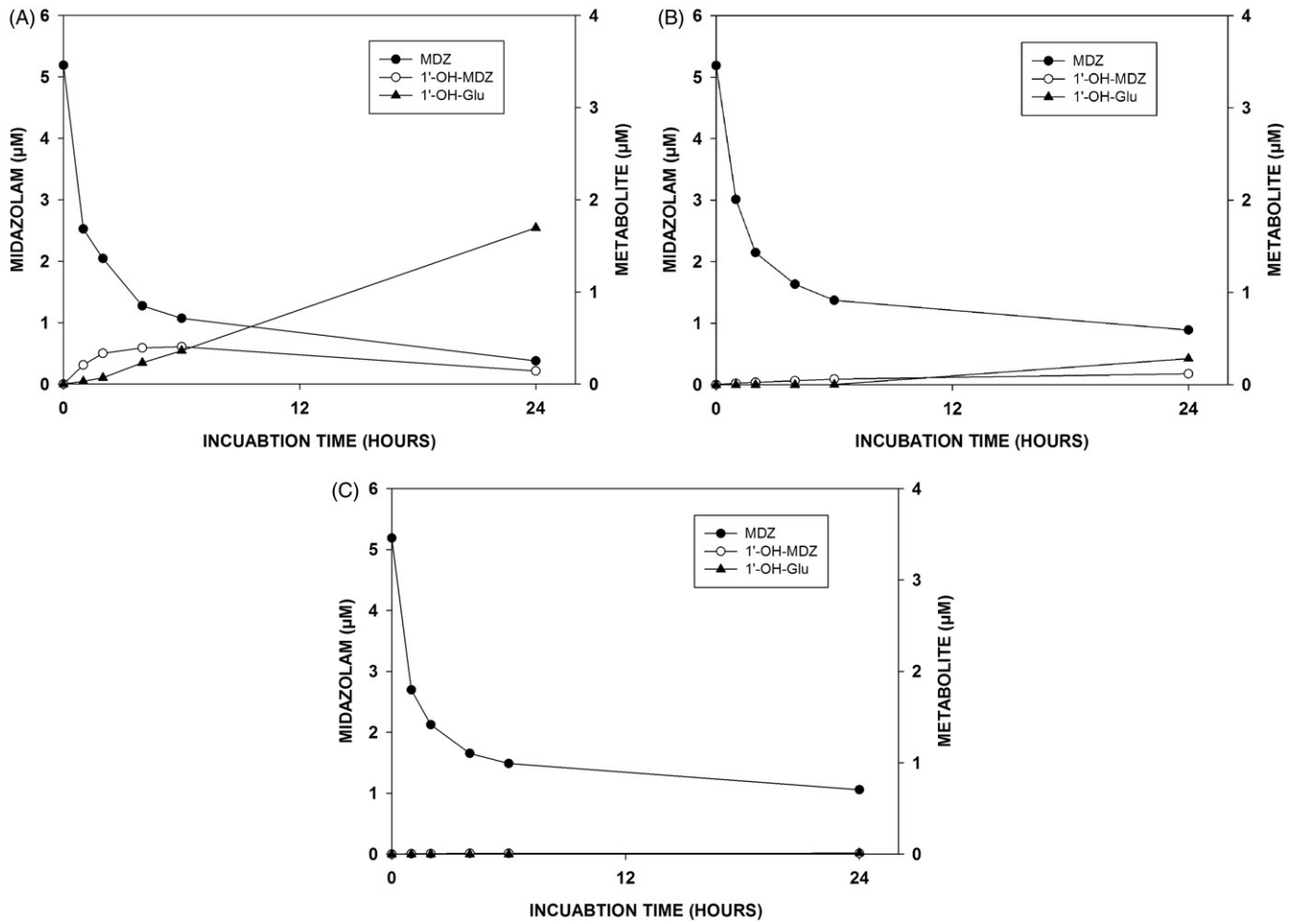

Figure 10. Kinetics of midazolam (MDZ), 1′-hydroxy-midazolam (1′-OH-MDZ), 1′-hydroxy-midazolam glucuronide (1′-OH-Glu) following incubation of human hepatocytes from preparation QHu4019 in dynamic LiverChip^{TM} conditions at Day 4 with 5 µM Midazolam, in the absence (A) or in the presence of CYP inhibitors: ketoconazole (B) or 1-aminobenzotriazole (C).

Discussion

Liver tissue engineering has been under investigation for more than several decades to establish *in vitro* systems for drug metabolism and toxicity evaluation. Since primary hepatocytes rapidly lose their phenotype after isolation, maintaining liver-specific functions *in vitro* has been a major goal of these studies (Allen & Bhatia, 2002). The development of microfluidic-based technologies coupled to three-dimensional culture is an approach to mimic *in vivo* hemodynamic processes and to provide cells an opportunity to form a large number of intracellular contacts (Inamdar & Borenstein, 2011). CN Bio innovations' current perfused multiwell device called LiverChip™ is based on innovative technology developed initially at Massachusetts Institute of Technology in Pr LG Griffith's group. Several publications have focused on the design of the device, the assessment of oxygen consumption and oxygen transport in the circulating culture medium as well as the assessment of phenotype and function in the perfused multiwell system (Domansky et al., 2010; Sivaraman et al., 2005).

In the present study we investigated the phenotype, the expression levels of 22 genes involved in drug metabolism and transport, and the metabolic capacity of primary human hepatocytes in the LiverChip™ system in comparison to these functionalities in 2D-static culture (''gold standard''). Viability of cultured human hepatocytes was evaluated over time by immunohistochemistry and electron microscopy as well as through studying the common morphological and functional features of human hepatocytes in the device, as previously demonstrated in rat liver cells by Powers et al. (2002). After 7 days of culture, human hepatocytes in the dynamic LiverChip™ system exhibited a high viability as confirmed by a high level of albumin secretion. Moreover, the presence of bile canaliculi with microvilli and cell junctions, observed under TEM, was consistent with the maintenance of a well differentiated phenotype and hepatic metabolic functions during at least one week of culture. Future experiments will focus on investigation, by IHC, of the polarization of hepatocytes within microtissue. Indeed, IHC staining of the multidrug resistance protein 1 (MDR1) and bile salt export pump (BSEP) should provide evidence of the formation of functional bile canaliculi within microtissue (Hoffmann et al., 2012; Messner et al., 2013).

After having established the viability and well-differentiated phenotype of human hepatocytes within the dynamic LiverChip™ device, our goal was to evaluate the ability to maintain basal mRNA expression of genes involved in drug metabolism and transport and to compare these levels with those obtained with human hepatocytes cultured under 2D-static conditions. As already widely described with human hepatocytes in 2D-static cultures, we have also observed (in-house data not shown) a down-regulation of mRNA levels of the main CYPs during 24–48 h post-adhesion (Hewitt et al., 2007; Rodriguez-Antona et al., 2002) associated with a decreased cellular viability after Day 3 of culture excluding performing long-term metabolic or toxicity studies.

In the dynamic LiverChip™ system, basal CYP mRNA expression levels were also down-regulated during the first 2 days of culture. Nevertheless, from Day 2 to Day 7, for most of the genes (except for *CYP2B6* and *UGT1A6*, which were persistently up-regulated and *OATP1B3* down-regulated in a moderate range), basal mRNA levels were conserved. These results confirmed that the flow is the main driver of gene expression maintenance as previously reported in the literature by Vinci et al. (2011) and Hoffmann et al. (2012). These authors, using human hepatocytes in microfluidic bioreactors, demonstrated that major cytochromes genes (*CYP1A2* and *CYP3A4*) were partially recovered once perfusion started and during a 7-day period conversely to 2D-static culture or sandwich static conditions. Functionality of CYPs has been demonstrated by investigating the metabolism of specific probe substrates for the main CYP isoforms, i.e. phenacetin (CYP1A2), bupropion (CYP2B6), tolbutamide (CYP2C9), dextromethorphan (CYP2D6) and midazolam (CYP3A). One of the major issues reported in the literature being the non-specific binding of compound on microfluidic biochips (Baudoin et al., 2013; Novik et al., 2010; Prot et al., 2011), preliminary studies have been performed in order to address this point. After 24 h incubation time, less than 20% of initial concentration of each of the five probes were bound under perfusion.

Regarding the metabolic activity in the device, similarly to Hμrel® biochips (Novik et al., 2010) and miniaturized bioreactor (Hoffmann et al., 2012), CYPs activities, in the LiverChip™ system, were functional and maintained over 7 days. Using the IDCCM box, Baudoin et al. (2013) also demonstrated some metabolic activity after 24 h of culture of primary hepatocytes in the microfluidic biochips despite strong adsorption of compounds on the device. We demonstrated, in three different donor preparations, after 4 days in culture in the dynamic LiverChip™ system, 7-fold and a 6-fold higher CYP1A2 and CYP3A activities, respectively. CYP2D6 activity was two-fold higher compared to 2D-static conditions after one day plating while CYP2B6 and CYP2C9 activities were conserved under microfluidic conditions at similar level to 2D-cultures. Moreover, to illustrate the maintenance of CYP activity over time, midazolam clearance was determined at Day 4 and Day 7 post-seeding and CYP3A activity was found similar during the period. Since the present studies have clearly demonstrated that hepatic viability and metabolic function are maintained for long periods of time in the LiverChip™ system, future experiments will evaluate the capacity of hepatocytes in this model to both clear low clearance compounds and generate *in vitro–in vivo* correlations. In addition, the data generated under dynamic conditions in the LiverChip™ model, such as intrinsic clearance and fractional metabolism, will be used to predict clinical outcome in order to compare the predictiveness of this model with that of the classical 2D-static approach. Nevertheless, with new chemical entities, especially with high lipophilic compounds that may strongly stick to the device, preliminary mandatory investigations will have to be launched in order to assess non-specific bindings to the device.

To investigate the potential to improve the metabolic capacity of hepatocytes under the dynamic conditions of the LiverChip™ system, additional experiments using hepatocytes in co-culture with NPC could also be launched. Indeed, *in vitro* models based on a co-culture of human primary

hepatocytes with NPC have been shown to display higher rates of metabolite formation when compared to those in either static co-cultures of primary hepatocytes and NPC or dynamic primary hepatocyte monocultures (Chao et al., 2009; Novik et al., 2010).

One additional potential application for *in vitro* systems that maintain metabolic function over relatively long periods of time is the prediction of hepatic injury (Dash et al., 2009; Kratschmar, 2013; Yeon, 2010). In this case, co-cultures of hepatocytes with other cell types such as Kuppfer cells or other NPCs (stellate or sinusoidal endothelial cells) could be relevant (Soldatow et al., 2013). This illustrates that there remains considerable scope to explore the potential of this 3D microfluidic model, LiverChip™ system.

Finally, few ''organ on a chip'' systems including lung, brain and gut are already available (Baker, 2011). Further perspectives currently under development, the so-called ''human-on-a-chip'' rely on the development of even more sophisticated 3D/dynamic systems allowing different organs to co-habit recapitulating an almost whole body (Huh et al., 2011). One can imagine with this kind of system allowing more accurate prediction of drug efficacy, toxicity, and pharmacokinetics to accelerate the drug development process.

Conclusion

This study proved the maintenance of the human hepatocyte phenotype in the LiverChip™ device by both, the characterization of the morphological behavior of the cells and the analysis of mRNA basal expression of 22 genes involved in drug metabolism and transport over a 7-day culture period. Drug metabolism studies of major CYPs demonstrated their functionality illustrating the potential of hepatocytes maintained in the dynamic LiverChip™ system to reproduce *in vivo* hepatic tissue function during at least 7 days of culture.

Acknowledgements

We thank Dr Emma Sceats and Dr David Hughes from CN Bio Innovations for leasing the LiverChip™ device used for the experiments.

Declaration of interest

The authors report no conflicts of interest. The authors alone are responsible for the content and writing of this article.

References

Allen JW, Bhatia SN. (2002). Improving the next generation of bioartificial liver devices. Semin Cell Dev Biol 13:447–54.

Baker M. (2011). Tissue models: a living system on a chip. Nature 471: 661–5.

Baudoin R, Prot JM, Nicolas G, et al. (2013). Evaluation of seven drug metabolisms and clearances by cryopreserved human primary hepatocytes cultivated in microfluidic biochips. Xenobiotica 43:140–52.

Bokhari M, Carnachan RJ, Cameron NR, Przyborski SA. (2007). Novel cell culture device enabling three-dimensional cell growth and improved cell function. Biochem Biophys Res Commun 354: 1095–100.

Chao P, Maguire T, Novik E, et al. (2009). Evaluation of a microfluidic based cell culture platform with primary human hepatocytes for the prediction of hepatic clearance in human. Biochem Pharmacol 78: 625–32.

Dash A, Inman W, Hoffmaster K, et al. (2009). Liver tissue engineering in the evaluation of drug safety. Expert Opin Drug Metab Toxicol 5: 1159–74.

Domansky K, Inman W, Serdy J, Griffith L. (2005). Perfused microreactors for liver tissue engineering. Conf Proc IEEE Eng Med Biol Soc 7:7490–2.

Domansky K, Inman W, Serdy J, et al. (2010). Perfused multiwell plate for 3D liver tissue engineering. Lab Chip 10:51–8.

Godoy P, Hewitt NJ, Albrecht U, et al. (2013). Recent advances in 2D and 3D in vitro systems using primary hepatocytes, alternative hepatocyte sources and non-parenchymal liver cells and their use in investigating mechanisms of hepatotoxicity, cell signaling and ADME. Arch Toxicol 87:1315–30.

Faucette SR, Hawke RL, Lecluyse EL, et al. (2000). Validation of bupropion hydroxylation as a selective marker of human cytochrome P450 2B6 catalytic activity. Drug Metab Dispos 28:1222–30.

Fiegel HC, Havers J, Kneser U, et al. (2004). Influence of flow conditions and matrix coatings on growth and differentiation of three-dimensionally cultured rat hepatocytes. Tissue Eng 10: 165–74.

Hesse LM, Venkatakrishnan K, Court MH, et al. (2000). CYP2B6 mediates the in vitro hydroxylation of bupropion: potential drug interactions with other antidepressants. Drug Metab Dispos 28: 1176–83.

Hewitt NJ, Lechón MJ, Houston JB, et al. (2007). Primary hepatocytes: current understanding of the regulation of metabolic enzymes and transporter proteins, and pharmaceutical practice for the use of hepatocytes in metabolism, enzyme induction, transporter, clearance, and hepatotoxicity studies. Drug Metab Rev 39:159–234.

Hoffmann SA, Müller-Vieira U, Biemel K, et al. (2012). Analysis of drug metabolism activities in a miniaturized liver cell bioreactor for use in pharmacological studies. Biotechnol Bioeng 109:3172–81.

Huh D, Hamilton GA, Ingber DE. (2011). From 3D cell culture to organs-on-chips. Trends Cell Biol 21:745–54.

Inamdar NK, Borenstein JT. (2011). Microfluidic cell culture models for tissue engineering. Curr Opin Biotechnol 22:681–9.

Georgoff I, Secott T, Isom HC. (1984). Effect of simian virus 40 infection on albumin production by hepatocytes cultured in chemically defined medium and plated on collagen and non-collagen attachment surfaces. J Biol Chem 259:9595–602.

Kaihara S, Kim S, Kim BS, et al. (2000). Survival and function of rat hepatocytes cocultured with nonparenchymal cells or sinusoidal endothelial cells on biodegradable polymers under flow conditions. J Pediatr Surg 35:1287–90.

Kratschmar DV, Messner S, Moritz W, Odermatt A. (2013). Characterization of a rat multi-cell type 3D-liver microtissue system. J Tissue Sci Eng 4:130–6.

Klieber S, Hugla S, Ngo R, et al. (2008). Contribution of the N-glucuronidation pathway to the overall in vitro metabolic clearance of midazolam in humans. Drug Metab Dispos 36:851–62.

LeCluyse EL, Witek RP, Andersen ME, Powers MJ. (2012). Organotypic liver culture models: meeting current challenges in toxicity testing. Crit Rev Toxicol 42:501–48.

Livak KJ, Schmittgen TD. (2001). Analysis of relative gene expression data using real-time quantitative PCR and the 22DDCT method. Methods 25:402–8.

Lutz JD, Isoherranen N. (2012). Prediction of relative in vivo metabolite exposure from in vitro data using two model drugs: dextromethorphan and omeprazole. Drug Metab Dispos 40:159–68.

Maguire TJ, Novik E, Chao P, et al. (2009). Design and application of microfluidic systems for in vitro pharmacokinetic evaluation of drug candidates. Curr Drug Metab 10:1192–9.

Meng Q. (2010). Three-dimensional culture of hepatocytes for prediction of drug-induced hepatotoxicity. Expert Opin Drug Metab Toxicol 6: 733–46.

Messner S, Agarkova I, Moritz W, Kelm JM. (2013). Multi-cell type human liver microtissues for hepatotoxicity testing. Arch Toxicol 87: 209–13.

Meyer A, Vuorinen A, Zielinska AE, et al. (2013). Formation of threohydrobupropion from bupropion is dependent on 11β-hydroxysteroid dehydrogenase 1. Drug Metab Dispos 41:1671–8.

Novik E, Maguire TJ, Chao P, et al. (2010). A microfluidic hepatic coculture platform for cell-based drug metabolism studies. Biochem Pharmacol 79:1036–44.

Powers MJ, Janigian DM, Wack KE, et al. (2002). Functional behavior of primary rat liver cells in a three-dimensional perfused microarray bioreactor. Tissue Eng 8:499–513.

Prot JM, Videau O, Brochot C, et al. (2011). A cocktail of metabolic probes demonstrates the relevance of primary human hepatocyte cultures in a microfluidic biochip for pharmaceutical drug screening. Int J Pharm 408:67–75.

Rodríguez-Antona C, Donato MT, Boobis A, et al. (2002). Cytochrome P450 expression in human hepatocytes and hepatoma cell lines: molecular mechanisms that determine lower expression in cultured cells. Xenobiotica 32:505–20.

Sivaraman A, Leach JK, Townsend S, et al. (2005). A microscale in vitro physiological model of the liver: predictive screens for drug metabolism and enzyme induction. Curr Drug Metab 6:569–91.

Soldatow VY, Lecluyse EL, Griffith LG, Rusyn I. (2013). In vitro models for liver toxicity testing. Toxicol Res 2:23–39.

Takashima T, Murase S, Iwasaki K, Shimida K. (2005). Evaluation of dextromethorphan metabolism using hepatocytes from CYP2D6 poor and extensive metabolizers. Drug Metab Pharmacokinet 20:177–82.

Vinci B, Duret C, Klieber S, et al. (2011). Modular bioreactor for primary human hepatocyte culture: medium flow stimulates expression and activity for detoxification genes. Biotechnol J 6:554–64.

Wang S, Nagrath D, Chen PC, et al. (2008). Three-dimensional primary hepatocyte culture in synthetic self-assembling peptide hydrogel. Tissue Eng 14:227–36.

Yeon JH, Na D, Park JK. (2010). Hepatotoxicity assay using human hepatocytes trapped in microholes of a microfluidic device. Electrophoresis 31:3167–74.

Supplementary material available online

Supplementary Figures S1–S3 and Tables S1 and S2